

Published in final edited form as:

Neuron. 2012 April 12; 74(1): 95–107. doi:10.1016/j.neuron.2012.02.022.

Intra-Axonal Translation of SMAD1/5/8 Mediates Retrograde Regulation of Trigeminal Ganglia Subtype Specification

Sheng-Jian Ji¹ and Samie R. Jaffrey^{1,*}

¹Department of Pharmacology, Weill Medical College, Cornell University, New York, NY 10065, USA

SUMMARY

In many cases, neurons acquire distinct identities as their axons navigate towards target cells and encounter target-derived signaling molecules. These molecules generate retrograde signals that activate subtype-specific gene transcription. Mechanisms by which axons convert the complex milieu of signaling molecules into retrograde signals are not fully understood. Here we examine retrograde signaling mechanisms that specify neuronal identity in the trigeminal ganglia, which relays sensory information from the face to the brain. We find that neuron specification requires the sequential action of two target-derived factors, BDNF and BMP4. BDNF induces the translation of axonally localized *SMAD1/5/8* transcripts. Axon-derived SMAD1/5/8 is translocated to the cell body, where it is phosphorylated to a transcriptionally active form by BMP4-induced signaling endosomes and mediates the transcriptional effects of target-derived BDNF and BMP4. Thus, local translation functions as a mechanism by which coincident signals are converted into a retrograde signal that elicits a specific transcriptional response.

INTRODUCTION

The nervous system is characterized by precise connectivity between neurons and specific target cells. A mechanism to ensure that neurons are matched to appropriate targets is by the differentiation of neurons into specific subtypes after their axons encounter inductive cues expressed in target fields during nervous system development (Hippenmeyer et al., 2004). The target-derived signaling molecules trigger the formation of incompletely understood signals that are propagated along the axon to the neuronal cell body. This form of retrograde signaling has been linked to changes in gene expression that lead to neuronal differentiation (Hippenmeyer et al., 2004; Nishi, 2003).

The embryonic trigeminal ganglion is a readily accessible system in which the interaction of target-derived factors and neuronal patterning has been explored (Davies, 1988). The trigeminal ganglion conveys sensory information from the face to somatosensory centers in the central nervous system. The trigeminal ganglion has three main peripheral axonal branches, the ophthalmic, maxillary, and mandibular, which innervate the corresponding regions of the face. Sensory information is then conveyed from the ganglia to the brainstem nuclei via a centrally projecting axonal bundle. The neurons that innervate each of these regions in the face are spatially segregated into specific domains within the ganglia and

© 2012 Elsevier Inc. All rights reserved

*Contact: srj2003@med.cornell.edu.

Publisher's Disclaimer: This is a PDF file of an unedited manuscript that has been accepted for publication. As a service to our customers we are providing this early version of the manuscript. The manuscript will undergo copyediting, typesetting, and review of the resulting proof before it is published in its final citable form. Please note that during the production process errors may be discovered which could affect the content, and all legal disclaimers that apply to the journal pertain.

exhibit distinct gene expression profiles, reflecting the division of these otherwise similar trigeminal neurons into distinct subtypes (Hodge et al., 2007). Some of these differentially expressed genes affect axonal pathfinding programs that allow the central projections of these neurons to innervate the brainstem (Hodge et al., 2007).

Studies on the mechanism of the acquisition of these distinct identities have focused on BMP4, a TGF- β family member expressed in the distal epithelium of the maxillary and ophthalmic regions in the face (Hodge et al., 2007). As axons grow into these regions, they encounter BMP4, which results in a retrograde signal that leads to nuclear accumulation of the phosphorylated and transcriptionally-active forms of the SMAD1, 5, and 8 transcription factors (Nohe et al., 2004). Additionally, *Tbx3*, a predicted SMAD1 target (Chen et al., 2008), is also selectively induced in the ophthalmic- and maxillary-innervating neurons in a BMP4-dependent manner (Hodge et al., 2007). This retrograde signaling contributes to the gene expression differences between the ophthalmic- and maxillary-innervating neurons and mandibular-innervating trigeminal neurons (Hodge et al., 2007). However, the nature of the retrograde BMP4 signal, and whether other factors are also involved in patterning the trigeminal ganglia remain unknown.

RESULTS

A Signaling Endosome Mechanism Mediates Retrograde BMP4 Signaling

We first sought to recapitulate retrograde BMP4 signaling in vitro by culturing dissociated E13.5 rat trigeminal ganglia neurons in microfluidic chambers (Taylor et al., 2005). In these devices, axons grow through a 450- μ m microgroove barrier and appear in the axonal compartment by 2 days in vitro (DIV). Because the axons are fluidically isolated from the cell bodies, this approach allows experimental treatments to be applied selectively to axons (Taylor et al., 2005) (Figure S1A, available online). The majority of the neurons that are adjacent to the microgrooves send an axon to the axonal compartment, as detected by retrograde labeling of cell bodies by axonal application of CM-DiI (Figure S1A).

Selective application of BMP4 to the axonal compartment resulted in an increase in nuclear pSMAD1/5/8 (Figures 1A and 1B; Figures S1B and S1C). pSMAD1/5/8 levels nearly doubled within 15 min, with further increases over 1–2 hr (Figure S1D). Total SMAD1/5/8 localization and levels were unaffected (Figures S1E and S1F), indicating that BMP4 increases the fraction of SMAD1/5/8 that is phosphorylated.

Retrograde BMP4 signaling also increased *Tbx3* expression at 4 hr (Figures 1A and 1C; Figures S1B and S1G), with further increases over a 24 hr period (data not shown). This delay in the appearance of *Tbx3* is consistent with a requirement for *Tbx3* transcription and translation following retrograde BMP4 signaling. Similar increases in pSMAD and *Tbx3* levels in the soma following axonal BMP4 treatment were also observed using Western blotting (Figures S1H and S1I). Notably, the retrograde signal generated by axonal application of BMP4 is as robust as BMP4 signals generated by activation of BMP4 receptors in the cell body, based on their similar ability to elevate pSMAD and *Tbx3* levels (Figures S1J and S1K).

We next asked if the retrograde signal is conveyed to the cell body by molecular motors. Application of the dynein inhibitor erythro-9-[3-(2-hydroxypropyl)] adenine (EHNA) (Penningroth, 1986) to the axonal compartment blocked the appearance of pSMAD1/5/8 and *Tbx3* induced by axonal application of BMP4 (Figures 1B and 1C). Furthermore, expression of dynamitin, which disassembles the dynactin complex required for dynein motor transport (Burkhardt et al., 1997), similarly blocked the increase in nuclear pSMAD by BMP4

treatments in axons (Figure 1D). Together, these data suggest that signaling molecules conveyed from distal axons in a dynein-dependent manner mediate axonal BMP4 signaling.

In the case of the neurotrophins, retrograde signaling has been shown to be mediated by “signaling endosomes” containing endocytosed receptors that are translocated in an active ligand-bound form to the cell body where they activate their effectors (Cosker et al., 2008; Ibanez, 2007). To test whether a similar mechanism may be involved in retrograde BMP4 signaling, we first asked whether the activity of BMP receptors is required in the cell body after axonal application of BMP4. Dorsomorphin, DMH2 and LDN193189, selective and reversible inhibitors of BMP type I receptors ALK2, ALK3 and ALK6, block BMP signaling, but not signaling by related TGF- β family members (Yu et al., 2008). Application of these inhibitors to the cell body blocked the increase in pSMAD1/5/8 and Tbx3 that was induced by application of BMP4 to axons (Figures 1B and 1C; Figures S1L–S1N). These data suggest that retrograde BMP4 signaling results in the appearance of active BMP4 receptors in the cell body, which is required for retrograde BMP4 signaling.

In these experiments, we confirmed that cell body levels of SMAD1/5/8 were unchanged (Figure S1F) and no signs of cytotoxicity were observed during the time course of the experimental treatments (Figure S1O). Local action of the inhibitor in the microfluidic chambers was also confirmed (Figure S1P).

To further test the idea that retrograde BMP4 signaling involves axonally derived activated BMP4 receptors, we monitored the translocation of BMP4 from the axon to the soma. Application of biotinylated BMP4 to the axonal compartment resulted in the appearance of biotin signals throughout the cell body, while biotinylated BSA failed to be retrogradely trafficked (Figure 1E) these data support a model in which axonal application of BMP4 elicits a retrograde signal that is translocated by dynein, and involves the appearance of both BMP4 and active BMP4 receptors in the cell body.

Requirement of Intra-Axonal mRNA Translation in Retrograde BMP4 Signaling

During the development of the nervous system, intra-axonal mRNA translation is a component of several signaling pathways, notably those involving axon guidance cues (Lin and Holt, 2008; Martin Ephrussi, 2009). We therefore asked if local protein synthesis is required for retrograde BMP4 signaling. Co-application of either of the translation inhibitors cycloheximide or anisomycin with BMP4 to axons substantially blocked retrograde BMP4 signaling (Figures 2A and 2B). The effect of axonal anisomycin treatment is not due to inhibition of protein synthesis in the cell body, as a labile control protein ODC in cell bodies is not affected (Figure S2A). In addition to inducing *Tbx3*, retrograde BMP4 signaling also leads to the repression of *OC1*, *OC2* and *Hmx1* in the cell body (Hodge et al., 2007). These effects were also blocked by axonal application of translation inhibitors (Figures 2C–2E).

We considered the possibility that inhibition of local translation could impair the retrograde translocation of BMP4 signaling endosomes. However, application of anisomycin to axons did not prevent the retrograde transport of biotinylated BMP4 (Figure S2B). Under these experimental conditions, the translation inhibitors did not elicit axonal or cell body toxicity compared to vehicle treatment (Figures S2C and S2D). Additionally, the effects of the protein synthesis inhibitors were not due to alterations in the levels of axonal BMPR1a, 1b and 2 or cell body SMAD1/5/8, or due to diffusion of the inhibitors into the cell body compartment (Figures S2E–J, S1F and S2K). These data indicate that translation of axonal mRNA(s) are required for retrograde BMP4 signaling.

SMAD 1, 5, and 8 mRNA and Protein Are Localized to Trigeminal Axons

To identify axonal mRNAs that may mediate retrograde BMP4 signaling, we considered proteins that are present in axons and may be translated locally. Although transcription factors are typically localized in the nucleus, previous studies have detected prominent labeling of phospho-SMAD1/5/8 (pSMAD1/5/8) in certain axonal branches of the trigeminal ganglia (Hodge et al., 2007). The axonal localization of these transcription factors raises the possibility that they are synthesized locally, and that this axonal pool of SMAD1/5/8 has a role in conveying retrograde patterning signals from target tissues.

Although pSMAD1/5/8 is selectively localized to ophthalmic and maxillary axons (Hodge et al., 2007), the absence of pSMAD1/5/8 immunoreactivity in mandibular axons could reflect the absence of SMAD phosphorylation in these axons, or the absence of SMAD protein altogether. Immunostaining using an anti-SMAD1/5/8 antibody shows labeling in the ophthalmic and maxillary axons, but not the mandibular axons (Figures 3A and S3A; data not shown), indicating that SMAD1/5/8 protein is absent from these axons.

To determine which isoform(s) are localized to trigeminal ganglia axons, we stained E13.5 rat trigeminal ganglia histological sections using isoform-specific antibodies. SMAD1, 5, and 8 labeling were found in both neuronal cell bodies and axons of the trigeminal ganglia (Figure 3B). Higher magnification images showed that SMAD1, 5 and 8 staining is specific, with labeling limited to neuronal cells co-labeled with the neuronal marker Isl1, but not in the surrounding non-neuronal cells (Figure S3B).

We next asked if *SMAD1*, *5*, or *8* transcripts are localized to trigeminal axons. As a first approach, we used RT-PCR of axonal mRNA. We prepared highly pure axonal preparations from trigeminal ganglia cultures using microfluidic chambers (Figure S3C). γ -*actin*, which has previously been shown to be excluded from axons (Bassell et al., 1998), was detected in cell body fractions, but not the axonal fraction by RT-PCR (Figure 3C). However, RT-PCR indicated that, β -*actin*, a well-characterized axonal mRNA (Olink-Coux and Hollenbeck, 1996), as well as *SMAD1*, *5*, and *8* mRNAs, were found in axons (Figure 3C).

Because SMAD1/5/8 protein is localized in maxillary and ophthalmic axons, but not mandibular axons, we asked if SMAD1/5/8 mRNA is also selectively localized to maxillary and ophthalmic axons. Despite the selective localization of SMAD1/5/8 protein, *SMAD1*, *5*, and *8* transcripts were found in axons of both maxillary/ophthalmic and mandibular subpopulations (Figure S3D), indicating that the difference in SMAD1/5/8 expression is not due to differences in RNA localization.

As a second approach, we examined the localization of *SMAD* isoform transcripts by fluorescence in situ hybridization (FISH). Riboprobes directed against either *SMAD1*, *5*, or *8*, as well as β -*actin*, exhibited punctate localization along the axon and in the growth cone of E13.5 DIV2 trigeminal neurons, while γ -*actin* and *Tbx3* mRNA, were not detected in axons (Figure 3D).

Axonal mRNAs have rarely been detected in tissue sections by in situ hybridization due to minimal axoplasmic volume, low levels of axonal mRNA, and the punctate and intermittent localization of axonal transcripts (Lin and Holt, 2008; Martin and Ephrussi, 2009). However, we detected clear and specific signals for each *SMAD* transcript along trigeminal axons in E12.5 mouse embryos (Figure S3E). The ability to detect *SMAD* transcripts in axons in tissue sections suggests that these mRNAs may be relatively abundant in trigeminal axons. Together, these data indicate that transcripts encoding SMAD1, 5, and 8 are found in the axons of trigeminal neurons.

Local Synthesis Contributes to Axonal SMAD1/5/8 Levels

We next sought to determine whether local translation contributes to SMAD levels in axons. As a first approach, we examined intra-axonal SMAD synthesis in E13.5 trigeminal neurons cultured in microfluidic chambers for 2 days. SMAD1/5/8 levels were measured by quantitative immunofluorescence, with background levels measured in SMAD1/5/8 knockdown neurons (Figures S4A–S4D). Application of anisomycin to the axonal compartment for 4 hr resulted in a 62.8% decrease in total axonal SMAD1/5/8 levels, compared to treatment with vehicle (Figure 4A; Figures S4E and S4F). Together, these data indicate that maintenance of SMAD1/5/8 levels requires intraaxonal protein synthesis.

As a second strategy to examine the source of axonal SMAD1/5/8, we performed FRAP (fluorescence recovery after photobleaching) analysis using a photoconvertible reporter of SMAD1 translation. Trigeminal neurons were transfected with a construct comprising the photoconvertible protein Dendra2 (Chudakov et al., 2007) fused to SMAD1, including its 3'UTR. The axons were severed after 2 days. By examining only severed axons, any possible contribution to axonal SMAD levels by anterograde SMAD transport from the cell body is eliminated. Dendra2-SMAD1-3'UTR^{SMAD1} was photobleached in distal axons. Following photobleaching, recovery of green fluorescent Dendra2-SMAD1 was detected within 10 min, with continued increases over 30 min (Figure 4B). This effect was completely blocked by treatment with anisomycin, indicating that local synthesis of SMAD1 accounts for the increase in Dendra2-SMAD1 in distal axons.

We next asked if anterograde transport from cell bodies substantially contributes to the levels of SMAD proteins in axons. Dendra2 or Dendra2-SMAD1 was expressed and photoconverted to the red fluorescent form in the cell body. The increase in red signals in distal axons was monitored over 60 min. Red fluorescent Dendra2-SMAD1 protein could not be detected in distal axons, while Dendra2 was readily detected (Figure S4G). These data further support that the idea that axonal SMAD is derived primarily from local synthesis, and not from transport from the cell body.

These experiments, as well as an additional approach using axon-specific knockdown of *SMAD1*, 5, and 8 mRNA (see Figure 6A, below), indicate that SMAD1/5/8 levels in axons are mainly dependent on local synthesis.

Axonal SMAD1/5/8 Traffics from Axons to Cell Bodies

The rapid decline in axonal SMAD1/5/8 levels following protein synthesis inhibition suggests that SMAD1/5/8 is rapidly turned over in axons. To determine the mechanism that leads to the loss of SMAD1/5/8 after protein synthesis inhibition, we examined SMAD1/5/8 levels in severed trigeminal axons. Severed axons can remain in culture for at least 2 hr before displaying signs of degeneration (Figure S5A). As expected, axonal SMAD1/5/8 levels dropped significantly upon axonal application of anisomycin (Figure 5A). However, the rapid decline in SMAD1/5/8 levels was not due to proteasomal degradation, since the proteasome inhibitor *N*-acetyl-L-leuciny-L-leucinal-L-norleucinal (LLnL), which prevents SMAD degradation (Gruendler et al., 2001), did not block the decline in axonal SMAD1/5/8 levels (Figure 5A).

We next considered the possibility that the loss in SMAD1/5/8 levels reflects retrograde trafficking of SMAD1/5/8 from distal axons. Consistent with this model, treatment of axons with the dynein inhibitor EHNA prevented the reduction of axonal SMAD1/5/8 after protein synthesis inhibition (Figure 5A; Figure S4E). Taken together, these data suggest that SMAD1/5/8 is transported retrogradely from distal axons in a motor-dependent manner.

To track the fate of axonally synthesized SMAD1/5/8, we used L-azidohomoalanine (AHA), a methionine analog that can be biotinylated using “click chemistry” (Kiick et al., 2002). E13.5 trigeminal ganglia neurons were cultured in microfluidic chambers, and AHA was added to the axonal compartment. AHA was allowed to incorporate into locally synthesized proteins, and the axonally synthesized, retrogradely trafficked proteins were collected by preparing lysates from the cell body compartment. pSMAD1/5/8 was immunoprecipitated and the presence of axonally derived AHA-labeled pSMAD1/5/8 was detected by anti-biotin Western blotting. Biotinylated pSMAD1/5/8 was observed in cell bodies with axons treated with BMP4 after immunoprecipitation and click reaction (Figure 5B). This effect was blocked by including anisomycin in the axon, demonstrating that the biotinylated pSMAD1/5/8 was synthesized in axons (Figure 5B). Together, these experiments show that endogenous, axonally derived SMAD1/5/8 is translocated to the cell body in its transcriptionally active phosphorylated form.

To further examine the retrograde trafficking of axonal SMAD, we imaged Dendra2-SMAD1 in axons. Dendra2 or Dendra2-SMAD1 was photoconverted to the red fluorescent form in the axon, and the distribution of the red signal was monitored over 50 s (Figure 5C). Red fluorescent Dendra2-SMAD1 preferentially localized to the proximal side of the photoconverted segment, consistent with the transport of SMAD protein in a retrograde manner (Figures S5B and S5C). The retrogradely transported Dendra2-SMAD1 accumulates in the nucleus as we detected a significant increase of red signal in the nucleus after photoconverting Dendra2-SMAD1 in axon (Figure 5D). Collectively these experiments suggest that axonal SMAD can be retrogradely trafficked back from the axon to the soma and accumulates in the nucleus.

BMP4 receptors typically bind to SMADs through adaptor proteins (Moustakas and Heldin, 2009; Shi et al., 2007). To determine if axonal SMAD associates with BMP4 receptors, we examined the localization of axonal SMAD1/5/8 with respect to signaling endosomes labeled with biotinylated BMP4. Following application of biotinylated BMP4 to the axonal compartment, biotinylated BMP4 exhibited significant colocalization with both axonal pSMAD1/5/8 and SMAD1/5/8 (Figure S5D), compared with biotinylated BSA. These data suggest that SMAD1/5/8 associates with BMP4 receptor complexes in axons.

Retrograde Gene Induction Requires Axonally Synthesized SMAD1/5/8

We next asked whether axonal SMAD is required for retrograde BMP4 signaling. To address this, we generated neurons with reduced *SMAD1/5/8* transcripts in axons using compartmentalized siRNA transfection (Hengst et al., 2006). We prepared two siRNA cocktails, each containing three siRNAs, one for each of the *SMAD1*, 5 and 8 isoforms. Transfection of either SMAD1/5/8 knockdown cocktail, but not the nontargeting control siRNA, into the axonal compartment resulted in significant reduction in axonal SMAD levels, measured using isoform-specific antibodies (Figures S6A–S6C) or using an antibody to SMAD1/5/8 (Figure 6A). Axonal transfection of either siRNA cocktail did not significantly affect transcript levels in cell bodies, as measured by *SMAD1*, 5 and 8 FISH analysis (Figures S6D–S6F). These results confirm that compartmentalized siRNA transfection only affected *SMAD1*, 5, 8 transcript levels in axons.

To determine if axonal SMAD mediates retrograde BMP4 signaling, we applied BMP4 to axons after compartmentalized knockdown of *SMAD1/5/8*. In these axonal SMAD1/5/8-deficient neurons, retrograde BMP4 signaling was significantly impaired, as measured by reduced induction of nuclear pSMAD1/5/8 and Tbx3 by axonal BMP4 treatment (Figures 6B and 6C; Figure S6G). No effect on retrograde trafficking of BMP4 endosomes was observed in axons transfected with the SMAD siRNA cocktail (Figure S6H). These data indicate that axonal SMAD is required for retrograde BMP4 signaling.

BDNF Induces Intra-Axonal SMAD1/5/8 Synthesis

Our finding that axonal SMAD1/5/8 mediates retrograde BMP4 signaling suggests that factors which regulate axonal synthesis of SMAD1, 5, and 8 would be required for proper patterning of the trigeminal ganglia. To screen for factors that induce SMAD1/5/8 synthesis, we examined SMAD1/5/8 levels in severed axons after application of different signaling molecules. Standard trigeminal ganglia neuron culturing media contains NT-3 and NGF. However, in this experiment, the axonal compartment of E13.5 trigeminal neurons was switched to neurotrophin- and BMP4-free media for 24 hr prior to severing. Notably, levels of axonal SMAD1/5/8 were essentially abolished 24 hr after switching to this media. We first asked if BMP4 induces SMAD1/5/8 in axons. However, treatment of axons with BMP4 did not increase SMAD1/5/8 levels significantly higher than background (Figures 7A and 7B).

We next considered the possibility that neurotrophins might regulate axonal SMAD levels, since these molecules have been shown to induce intra-axonal protein synthesis (Cox et al., 2008; Hengst et al., 2009; Yao et al., 2006; Zhang and Poo, 2002). Application of NGF did not induce a significant increase in axonal SMAD levels, while application of NT-3 caused a small, but significant increase in axonal SMAD levels (Figures 7A and 7B). However, despite the effect of NT-3, it is unlikely to be the major physiological regulator of axonal SMAD1/5/8 synthesis since NT-3 is expressed in the ophthalmic, maxillary, and mandibular regions of the face (Arumae et al., 1993; O'Connor and Tessier-Lavigne, 1999), while axonal SMAD1/5/8 is detected only in axons innervating the ophthalmic and maxillary regions (see Figures 3A and S3A).

Therefore, we next considered BDNF, which exhibits a highly specific ophthalmic and maxillary epidermal expression pattern, with no detectable levels in the mandibular region of the face (Arumae et al., 1993; O'Connor and Tessier-Lavigne, 1999). Application of BDNF to severed axons caused a 1.7-fold increase in axonal SMAD levels in 30 min (Figures 7A and 7B). This increase was blocked by co-application of anisomycin, indicating that axonal SMAD induction by BDNF is local synthesis-dependent (Figures 7A and 7B). As a control, Tau1 and TrkB receptor levels were not affected by these treatments (Figures S7A–S7C). These data indicate that neurotrophins, especially BDNF, induce SMAD expression in axons via local protein synthesis.

Retrograde Gene Induction Requires Coordinated Actions of BDNF and BMP4

Our data indicate that retrograde induction of nuclear pSMAD1/5/8 and Tbx3 requires target-derived BDNF-dependent intra-axonal synthesis of SMADs. Previous studies suggested that BMP4 was the primary regulator of pSMAD1/5/8 induction (Hodge et al., 2007). However, these experiments utilized bath application of BMP4, which results in activation of BMP4 receptors primarily on cell bodies. Because cell bodies express SMAD1/5/8 even in the absence of neurotrophins (Figure 3B), these studies do not address signaling in axons, which express SMAD1/5/8 only in the presence of neurotrophins. To test the idea that both BMP4 and neurotrophins are required for retrograde signaling, we cultured E13.5 trigeminal ganglia neurons in microfluidic chambers, and after 2 days switched the media to neurotrophin-free media for 4 hr. Under these modified culture conditions, axonal application of BMP4 for 1 hr failed to elicit retrograde induction of nuclear pSMAD1/5/8 (Figure 7C). Similarly, axonal application of BDNF for 1 hr was unable to induce nuclear pSMAD1/5/8. However, co-application of BDNF and BMP4 resulted in retrograde induction of nuclear pSMAD1/5/8 (Figure 7C). In each of these treatments, total cell body SMAD1/5/8 levels were not significantly affected (Figure S7D). These data indicate that BMP4 is not sufficient for retrograde signaling, but requires collaboration with neurotrophins.

To determine whether the induction of pSMAD1/5/8 and *Tbx3* by axonally applied BDNF also requires a retrogradely trafficked TrkB signaling endosome, we used the Trk inhibitor K252a (Tapley et al., 1992). Application of K252a to axons of E13.5 trigeminal ganglia neurons in microfluidic chambers blocked the ability of axonally applied BDNF and BMP4 to induce *Tbx3*, without affecting retrograde transport of BMP4 signaling endosomes (Figure 7D; Figure S7E). These data indicate that the effects of BDNF in mediating retrograde BMP4 signaling reflect local, intra-axonal actions of BDNF and do not require the activity of Trk receptors in the cell body. Together, these data indicate that BDNF and BMP4 receptors have roles in distinct compartments within the neuron to mediate retrograde signaling. BDNF is required within the axon, where it acts to regulate intra-axonal SMAD1/5/8 synthesis, while axonal application of BMP4 induces the appearance of BMP4 receptor activity in the cell body.

Target-Derived BDNF Regulates Axonal SMAD1/5/8 Expression and the Acquisition of Positional Identity Markers during Trigeminal Ganglia Development

We next wanted to assess whether target-derived BDNF has a physiological role in regulating the levels of SMAD1/5/8 in axons in developing embryos. During early embryonic development, BDNF expression is principally localized to the maxillary and ophthalmic mesenchyme, with highest expression toward the epithelium, but is absent from the mandibular mesenchyme (Arumae et al., 1993; O'Connor and Tessier-Lavigne, 1999). The absence of BDNF in the mandibular mesenchyme matches with the absence of SMAD1/5/8 from the mandibular branch in E12.5 mouse embryos (Figures 3A and S3A). This correspondence suggests a causal role for BDNF in controlling axonal SMAD1/5/8 levels in vivo.

To determine if BDNF physiologically regulates axonal SMAD levels, we examined axonal SMAD levels in maxillary and ophthalmic axons of the trigeminal ganglia in E12.5 *BDNF*^{-/-} mouse embryos. *BDNF*^{-/-} embryos exhibit normal trigeminal ganglion development, as well as normal trigeminal axon growth and pathfinding in early embryonic development (Ernfors et al., 1994; O'Connor and Tessier-Lavigne, 1999). While SMAD1/5/8 was readily detectable in maxillary axons of *BDNF*^{+/-} littermate control embryos, axonal SMAD1/5/8 levels were markedly reduced in *BDNF*^{-/-} embryos (Figure 8A; Figures S8A–S8C). Similarly, SMAD1/5/8 levels were markedly reduced in the ophthalmic bundle in *BDNF*^{-/-} embryos compared to *BDNF*^{+/-} littermate controls (Figure S8D). These data suggest that target-derived BDNF physiologically regulates the expression of SMAD1/5/8 in axons.

Our experiments using cultured neurons suggest that BDNF promotes the ability of BMP4 to retrogradely induce the expression of *Tbx3*, a positional identity marker for maxillary/ophthalmic trigeminal neurons. To further examine this idea, we asked whether mandibular neurons can be induced to express maxillary/ophthalmic positional identity markers. Explants derived from either the maxillary/ophthalmic or the mandibular portion of E13.5 rat trigeminal ganglia were cultured in microfluidic chambers. Application of BDNF/BMP4 to the axonal compartment led to *Tbx3* expression in both maxillary/ophthalmic and mandibular explants (Figure S8E). These results suggest that the mandibular neurons have the capacity to express maxillary/ophthalmic positional identity markers, but most likely do not because they are not physiologically exposed to BDNF and BMP4.

To address the physiological role of BDNF in regulating the patterning of the trigeminal ganglia, we examined positional identity markers in *BDNF*^{-/-} embryos. In E12.5 control (*BDNF*^{+/-}) embryos, pSMAD1/5/8 and *Tbx3* are highly expressed in the nuclei of maxillary- and ophthalmic-innervating neurons of the trigeminal ganglia (Figure 8B). However, in *BDNF*^{-/-} embryos, nuclear pSMAD1/5/8 and *Tbx3* staining in the ophthalmic

and maxillary regions of the trigeminal ganglia is reduced to levels seen in the mandibular region of the trigeminal ganglia (Figures 8B–8D). The loss of nuclear pSMAD and Tbx3 signals reflects reduced expression levels, not the loss of neurons, since neuronal number, as measured by Isl1 staining, is unaffected (Figure 8B). These data indicate that target-derived BDNF is critical for the acquisition of positional identity markers in the trigeminal ganglia.

We considered the possibility that the induction of the positional identity markers was delayed in *BDNF*^{-/-} embryos. However, *Tbx3* expression was also absent at E13.5 (Figures 8B). As an additional control, we examined whether BMP4 expression was affected in *BDNF*^{-/-} embryos. Immunostaining of BMP4 in the face was essentially identical in *BDNF*^{+/-} and *BDNF*^{-/-} embryos (Figure S8F), indicating that impaired expression of positional identity markers in the trigeminal ganglia cannot be attributed to reduced expression of BMP4 in *BDNF*^{-/-} embryos. Lastly, we addressed whether *SMAD* transcript expression levels are affected in *BDNF*^{-/-} embryos. In situ hybridization shows that *SMAD1*, 5 and 8 expression was unaffected in *BDNF*^{-/-} embryos (Figure S8G), suggesting that reduced pSMAD in neuronal nuclei and SMAD in axons is not due to impaired *SMAD* transcription. Together, these data indicate that BDNF is a target-derived factor that physiologically regulates axonal SMAD1/5/8 levels and is required for patterning the trigeminal ganglia.

DISCUSSION

Although combinations of distinct inductive cues are critical for the specification of early neuronal types from neuronal progenitors, it has not previously been known if multiple inductive cues also act on axons to specify neuronal identity. In this case, distal axons will require mechanisms to generate retrograde signals that reflect the simultaneous detection of multiple cues. We find that retrograde patterning of the trigeminal ganglia requires both BMP4 and BDNF, and that both signals act on distal axons to generate a retrograde signal. Our results identify local translation as a mechanism that allows the axon to elicit a retrograde signal only upon detection of both target-derived factors. We find that *SMAD1*, 5, and 8 transcripts are localized to trigeminal ganglia axons, and that these mRNAs are selectively translated in response to BDNF. Axonal SMAD1/5/8 is then retrogradely trafficked to the cell body, along with BMP4 signaling endosomes, to regulate target gene transcription in the maxillary and ophthalmic neuron subsets of the trigeminal ganglia (Figure S8H). In this manner, intra-axonal translation provides a mechanism by which spatially and temporally coincident target-derived signals are processed to obtain specific responses, by limiting retrograde BMP4 signaling to regions that also contain BDNF.

Our results also identify a new mechanism by which the transcription factor repertoire of neuronal subtypes is determined. Transcription factors have a central role in defining the identity of neuronal subtypes, with the expression of specific combinations of transcription factors linked to aspects of neuronal pathfinding, connectivity, and function (Dasen and Jessell, 2009; Narita and Rijli, 2009). In most cases, transcription factors involved in patterning are induced by morphogenic cues. Here we show that the transcription factors that regulate neuronal identity can be stored in a latent form as axonally localized transcripts, which are locally translated in response to specific target-derived signals. These axonal transcription factors are retrogradely trafficked to induce the gene expression programs regulating neuronal fate and identity. Our data raise the intriguing possibility that the local translation and retrograde trafficking of transcription factors may be a recurrent feature in neuronal subtype specification and patterning.

We find that BDNF and BMP4 have distinct and sequential roles in retrograde signaling. Following BDNF-induced SMAD1/5/8 synthesis in axons, BMP4 signaling is required for the transcriptional activity of axonally derived SMAD1/5/8 in the cell body. The axonally derived SMAD1/5/8 pool may be a preferential target for BMP4 signaling endosomes because of the manner in which BMP4 receptors phosphorylate their targets. BMP4 receptors preferentially phosphorylate SMADs that they are directly coupled to via adaptor proteins such as endofin (Moustakas and Heldin, 2009; Shi et al., 2007). Indeed, we find that SMAD1/5/8 is colocalized with BMP4 signaling endosomes in axons, suggesting direct phosphorylation of axonally derived SMAD1/5/8. Consistent with this idea, SMAD1/5/8 is present in a phosphorylated form in axons (Hodge et al., 2007), confirming direct regulation of SMADs in axons. Since phosphorylation is a labile modification that is readily reversed by phosphatases, mechanisms must exist to maintain SMAD1/5/8 in a phosphorylated form. The cotrafficking of SMAD1/5/8 with BMP4 signaling endosomes may serve to maintain SMADs in a phosphorylated form during retrograde trafficking, and once the axonally derived SMAD1/5/8 enters the cell body.

The initial discovery of robust staining of pSMAD1/5/8 in axons raised the question about the functional role for this localization (Hodge et al., 2007). The relatively robust staining of SMAD1/5/8 that we found in axons suggests that the overall levels of pSMAD1/5/8 derived from the axonal pool may be sufficient to exert a transcriptional effect in trigeminal neurons. Additionally, other axon-specific modifications of SMAD1/5/8 may also influence the transcriptional activity of axonal SMAD1/5/8. Although axonal SMAD promotes retrograde BMP4 signaling, it is possible that preexisting SMAD1/5/8 in the cell body may have access to BMP4 signaling endosomes and contribute to overall retrograde signaling. Additionally, other local translation events may also promote retrograde signaling.

Although roles for intra-axonal translation have been well studied in vitro, there is limited evidence for the physiological significance of intra-axonal translation. Thus, data showing that the localization of endogenous protein to axons is due to local synthesis in vivo is lacking. The phenotype of the *BDNF*^{-/-} mouse provides evidence for the physiological significance for the intra-axonal translation of SMAD1/5/8. *BDNF*^{-/-} mice display a selective loss of SMAD1/5/8 from axons. This loss in axonal SMAD1/5/8 is consistent with BDNF-dependent regulation of SMAD1/5/8 translation in axons. The physiological importance of axonal SMAD is suggested by the markedly reduced pSMAD1/5/8 and Tbx3 levels in the nucleus of ophthalmic and maxillary-innervating neurons of the trigeminal ganglia of *BDNF*^{-/-} mice, phenocopying the *BMP4*^{-/-} mouse (Hodge et al., 2007).

The physiological importance of BDNF in regulating axonal synthesis of SMAD1/5/8 is also supported by the absence of SMAD1/5/8 in the mandibular axons in wild-type embryos. Although all the trigeminal axonal populations contain *SMAD1/5/8* transcripts, the protein is selectively expressed in the ophthalmic and maxillary axons, which encounter BDNF in target tissues. The absence of SMAD1/5/8 from mandibular axons is likely due to the failure of these axons to encounter BDNF in the mandibular target field.

Numerous other examples of neuronal subtype specification and patterning have been linked to signaling by target-derived factors (Chao et al., 2009; Hippenmeyer et al., 2004; Nishi, 2003). Coincident detection of multiple target-derived factors may be an important mechanism to specifically delineate specific neuronal pools. Indeed, another potential role for coincidence detection is suggested by the finding that sensory neuron specification is influenced by the combination of activin A, a TGF- β family member, and NGF, a neurotrophin (Xu and Hall, 2007). Together, the findings in our study identify a novel coincidence detector mechanism that allows axons to resolve complex patterns of target-derived factors to control retrograde signaling involved in neuronal specification.

EXPERIMENTAL PROCEDURES

Neuronal Culture

Trigeminal ganglia harvested from E13.5 rat embryos were dissected and cultured as reported previously (Ernfors et al., 1994). Expression constructs were nucleofected (Amaxa) into E13.5 trigeminal neurons following the manufacturer's instructions.

Microfluidic Chamber Assays

Microfluidic chambers were prepared as described previously (Taylor et al., 2005). The dissociated trigeminal neurons were plated in the cell body compartment (see Figure S1A). After culturing for 2–3 DIV, axons typically have grown across the microgrooves to the axonal compartment. Treatments can be applied specifically to either axonal compartment or cell body compartment. Details of microfluidic chamber experiments can be found in the Supplemental Information.

Immunostaining, Immunohistochemistry and In Situ Hybridization

For all immunofluorescence experiments using cultured neurons in microfluidic chambers, trigeminal neuron cell bodies and axons were fixed with 4% paraformaldehyde (PFA)/phosphate-buffered saline (PBS), pH 7.4. For immunohistochemistry, embryos were dissected, fixed and sectioned as described previously (Ji et al., 2009). TUNEL assay was carried out as described (ApoAlert DNA Fragmentation Assay Kit, Clontech). In situ hybridization on mouse sections using DIG-labeled RNA probes was performed as described (Schaeren-Wiemers and Gerfin-Moser, 1993). Fluorescence in situ hybridization (FISH) in cultured trigeminal axons was carried out as reported (Vessey et al., 2008). Fluorescent images were collected using a LSM 510 Zeiss laser-scanning confocal microscope. Image collection, quantification and statistical methods are described in the Supplemental Information. For colocalization analysis, Manders colocalization coefficients were calculated using Fiji/ImageJ (Coloc 2 plugin).

Axonal RNA RT PCR

E13.5 rat trigeminal neurons were cultured in 10 microfluidic chambers (Taylor et al., 2005) (see Figure S3C) per replicate for 3 days. RNA was harvested by applying 50 μ l TRIZOL (Invitrogen) to either the axonal or cell body compartment. Detailed protocols for axonal RNA RT-PCR can be found in the Supplemental Information.

Live Cell Imaging and Photoconversion of Trigeminal Neurons

Dissociated E13.5 trigeminal neurons were nucleofected with pDendra2-SMAD1-3'UTR^{SMAD1} and pDendra2. For details on FRAP, retrograde and anterograde trafficking experiments, see the Supplemental Information.

Click Chemistry

E13.5 rat trigeminal neurons were cultured in microfluidic chambers for 2 days before replacing the media with methionine-free media containing Click-iT AHA (L-azidohomoalanine, 50 μ M) (Invitrogen) in the axonal compartment. pSMAD1/5/8 was immunoprecipitated and the click reaction was carried out on the immunoprecipitate using Click-iT Protein Reaction Buffer Kit (Invitrogen) and biotin-alkyne (40 μ M) according to the manufacturer's instructions. For details, see the Supplemental Information.

Knockdown Using siRNA and shRNA

siRNA-mediated knockdown of *SMAD1*, 5 and 8 mRNAs in axons were carried out using GeneSilencer siRNA Transfection Reagent (Genlantis) as described previously (Hengst et al., 2006; Hengst et al., 2009). shRNA against receptors were designed using OligoEngine Workstation and constructs were made in pSUPER.GFP vector (OligoEngine). pSUPER.GFP.shRNA constructs were introduced into trigeminal neurons by nucleofection. Target sequences and detailed experimental designs can be found in the Supplemental Information.

Supplementary Material

Refer to Web version on PubMed Central for supplementary material.

Acknowledgments

We thank members of the Jaffrey lab for comments and suggestions, F. Lee (Weill Cornell Medical College) for *BDNF* mutant mice, K. A. Lukyanov (Russian Academy of Sciences) for the pDendra2 plasmid, C. C. Hong (Vanderbilt University) for DMH2 and LDN193189, S. Bhuvanendran, M. Marchand, S. Galdeen and A. North (Bio-Imaging Resource Center, The Rockefeller University) for help with confocal and DeltaVision microscopy and suggestions on image quantification, and N. L. Jeon and J. Harris (University of California, Irvine) for designing microfluidic chambers and for advice on their preparation and use. Supported by a Klingenstein Fellowship award in the Neurosciences (S.R.J.) and by NINDS grant R01 MH080420.

REFERENCES

- Arumae U, Pirvola U, Palgi J, Kiema TR, Palm K, Moshnyakov M, Ylikoski J, Saarma M. Neurotrophins and their receptors in rat peripheral trigeminal system during maxillary nerve growth. *J Cell Biol.* 1993; 122:1053–1065. [PubMed: 8354693]
- Bassell GJ, Zhang H, Byrd AL, Femino AM, Singer RH, Taneja KL, Lifshitz LM, Herman IM, Kosik KS. Sorting of β -actin mRNA and protein to neurites and growth cones in culture. *Journal of Neuroscience.* 1998; 18:251–265. [PubMed: 9412505]
- Burkhardt JK, Echeverri CJ, Nilsson T, Vallee RB. Overexpression of the dynamitin (p50) subunit of the dynactin complex disrupts dynein-dependent maintenance of membrane organelle distribution. *J Cell Biol.* 1997; 139:469–484. [PubMed: 9334349]
- Chao DL, Ma L, Shen K. Transient cell-cell interactions in neural circuit formation. *Nat Rev Neurosci.* 2009; 10:262–271. [PubMed: 19300445]
- Chen X, Xu H, Yuan P, Fang F, Huss M, Vega VB, Wong E, Orlov YL, Zhang W, Jiang J, et al. Integration of external signaling pathways with the core transcriptional network in embryonic stem cells. *Cell.* 2008; 133:1106–1117. [PubMed: 18555785]
- Chudakov DM, Lukyanov S, Lukyanov KA. Tracking intracellular protein movements using photoswitchable fluorescent proteins PS-CFP2 and Dendra2. *Nat Protoc.* 2007; 2:2024–2032. [PubMed: 17703215]
- Cosker KE, Courchesne SL, Segal RA. Action in the axon: generation and transport of signaling endosomes. *Curr Opin Neurobiol.* 2008; 18:270–275. [PubMed: 18778772]
- Cox LJ, Hengst U, Gurskaya NG, Lukyanov KA, Jaffrey SR. Intra-axonal translation and retrograde trafficking of CREB promotes neuronal survival. *Nature Cell Biology.* 2008; 10:149–159.
- Dasen JS, Jessell TM. Hox networks and the origins of motor neuron diversity. *Curr Top Dev Biol.* 2009; 88:169–200. [PubMed: 19651305]
- Davies AM. The trigeminal system: an advantageous experimental model for studying neuronal development. *Development.* 1988; 103(Suppl):175–183. [PubMed: 3074907]
- Ernfors P, Lee KF, Jaenisch R. Mice lacking brain-derived neurotrophic factor develop with sensory deficits. *Nature.* 1994; 368:147–150. [PubMed: 8139657]
- Gruendler C, Lin Y, Farley J, Wang T. Proteasomal degradation of Smad1 induced by bone morphogenetic proteins. *J Biol Chem.* 2001; 276:46533–46543. [PubMed: 11571290]

- Hengst U, Cox LJ, Macosko EZ, Jaffrey SR. Functional and selective RNA interference in developing axons and growth cones. *J Neurosci*. 2006; 26:5727–5732. [PubMed: 16723529]
- Hengst U, Deglincerti A, Kim HJ, Jeon NL, Jaffrey SR. Axonal elongation triggered by stimulus-induced local translation of a polarity complex protein. *Nat Cell Biol*. 2009; 11:1024–1030. [PubMed: 19620967]
- Hippenmeyer S, Kramer I, Arber S. Control of neuronal phenotype: what targets tell the cell bodies. *Trends Neurosci*. 2004; 27:482–488. [PubMed: 15271496]
- Hodge LK, Klassen MP, Han BX, Yiu G, Hurrell J, Howell A, Rousseau G, Lemaigre F, Tessier-Lavigne M, Wang F. Retrograde BMP Signaling Regulates Trigeminal Sensory Neuron Identities and the Formation of Precise Face Maps. *Neuron*. 2007; 55:572–586. [PubMed: 17698011]
- Ibanez CF. Message in a bottle: long-range retrograde signaling in the nervous system. *Trends Cell Biol*. 2007; 17:519–528. [PubMed: 18029183]
- Ji SJ, Periz G, Sockanathan S. Nolz1 is induced by retinoid signals and controls motoneuron subtype identity through distinct repressor activities. *Development*. 2009; 136:231–240. [PubMed: 19056829]
- Kiick KL, Saxon E, Tirrell DA, Bertozzi CR. Incorporation of azides into recombinant proteins for chemoselective modification by the Staudinger ligation. *Proc Natl Acad Sci U S A*. 2002; 99:19–24. [PubMed: 11752401]
- Lin AC, Holt CE. Function and regulation of local axonal translation. *Curr Opin Neurobiol*. 2008; 18:60–68. [PubMed: 18508259]
- Martin KC, Ephrussi A. mRNA localization: gene expression in the spatial dimension. *Cell*. 2009; 136:719–730. [PubMed: 19239891]
- Moustakas A, Heldin CH. The regulation of TGFbeta signal transduction. *Development*. 2009; 136:3699–3714. [PubMed: 19855013]
- Narita Y, Rijli FM. Hox genes in neural patterning and circuit formation in the mouse hindbrain. *Curr Top Dev Biol*. 2009; 88:139–167. [PubMed: 19651304]
- Nishi R. Target-mediated control of neural differentiation. *Prog Neurobiol*. 2003; 69:213–227. [PubMed: 12757747]
- Nohe A, Keating E, Knaus P, Petersen NO. Signal transduction of bone morphogenetic protein receptors. *Cell Signal*. 2004; 16:291–299. [PubMed: 14687659]
- O'Connor R, Tessier-Lavigne M. Identification of maxillary factor, a maxillary process-derived chemoattractant for developing trigeminal sensory axons. *Neuron*. 1999; 24:165–178. [PubMed: 10677035]
- Olink-Coux M, Hollenbeck PJ. Localization and active transport of mRNA in axons of sympathetic neurons in culture. *Journal of Neuroscience*. 1996; 16:1346–1358. [PubMed: 8778286]
- Penningroth SM. Erythro-9-[3-(2-hydroxynonyl)]adenine and vanadate as probes for microtubule-based cytoskeletal mechanochemistry. *Methods Enzymol*. 1986; 134:477–487. [PubMed: 2950298]
- Schaeren-Wiemers N, Gerfin-Moser A. A single protocol to detect transcripts of various types and expression levels in neural tissue and cultured cells: in situ hybridization using digoxigenin-labelled cRNA probes. *Histochemistry*. 1993; 100:431–440. [PubMed: 7512949]
- Shi W, Chang C, Nie S, Xie S, Wan M, Cao X. Endofin acts as a Smad anchor for receptor activation in BMP signaling. *J Cell Sci*. 2007; 120:1216–1224. [PubMed: 17356069]
- Tapley P, Lamballe F, Barbacid M. K252a is a selective inhibitor of the tyrosine protein kinase activity of the trk family of oncogenes and neurotrophin receptors. *Oncogene*. 1992; 7:371–381. [PubMed: 1312698]
- Taylor AM, Blurton-Jones M, Rhee SW, Cribbs DH, Cotman CW, Jeon NL. A microfluidic culture platform for CNS axonal injury, regeneration and transport. *Nature Methods*. 2005; 2:599–605. [PubMed: 16094385]
- Vessey JP, Macchi P, Stein JM, Mikl M, Hawker KN, Vogelsang P, Wiczorek K, Vendra G, Riefler J, Tubing F, et al. A loss of function allele for murine Staufin1 leads to impairment of dendritic Staufin1-RNP delivery and dendritic spine morphogenesis. *Proc Natl Acad Sci U S A*. 2008; 105:16374–16379. [PubMed: 18922781]

- Xu P, Hall AK. Activin acts with nerve growth factor to regulate calcitonin gene-related peptide mRNA in sensory neurons. *Neuroscience*. 2007; 150:665–674. [PubMed: 17964731]
- Yao J, Sasaki Y, Wen Z, Bassell GJ, Zheng JQ. An essential role for beta-actin mRNA localization and translation in Ca²⁺-dependent growth cone guidance. *Nat Neurosci*. 2006; 9:1265–1273. [PubMed: 16980965]
- Yu PB, Hong CC, Sachidanandan C, Babitt JL, Deng DY, Hoyng SA, Lin HY, Bloch KD, Peterson RT. Dorsomorphin inhibits BMP signals required for embryogenesis and iron metabolism. *Nat Chem Biol*. 2008; 4:33–41. [PubMed: 18026094]
- Zhang X, Poo MM. Localized synaptic potentiation by BDNF requires local protein synthesis in the developing axon. *Neuron*. 2002; 36:675–688. [PubMed: 12441056]

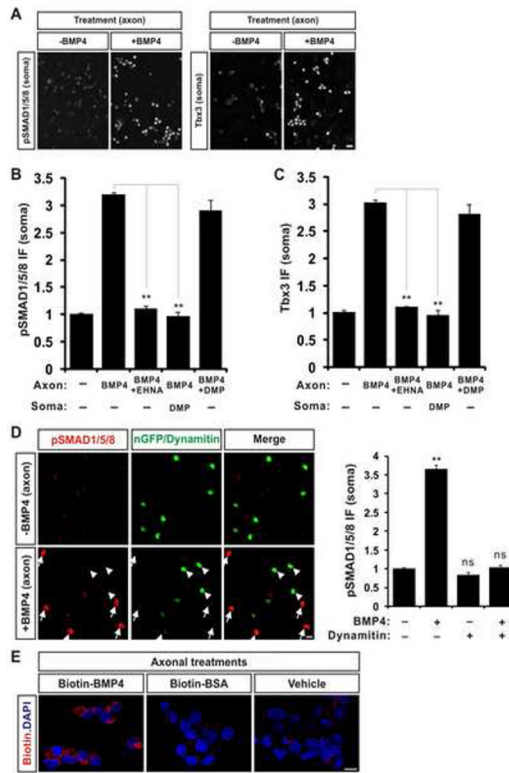


Figure 1. A Signaling Endosome Mechanism Mediates Retrograde BMP4 Signaling

(A) Axonal application of BMP4 induces increases in nuclear pSMAD1/5/8 and Tbx3 levels. Dissociated E13.5 trigeminal ganglia neurons were cultured in microfluidic chambers for 2 DIV, to allow axons to cross to the axonal compartment. Application of BMP4 (20 ng/ml) to the axonal compartment leads to an increase in pSMAD1/5/8 and Tbx3 levels in the nuclei of trigeminal neurons. Shown are anti-pSMAD1/5/8 and anti-Tbx3 immunostaining of neurons following axonal application of BMP4 for 1 hr (pSMAD1/5/8) and 4 hr (Tbx3), respectively.

(B and C) The BMP4 retrograde signal is conveyed by molecular motors and requires BMP4 receptor activity in the cell body. BMP4 treatment in axons induced a 2.2-fold increase in pSMAD1/5/8 (B) and a 2.0-fold increase in Tbx3 (C) immunofluorescence intensity in cell bodies. This effect was blocked by co-application of the retrograde motor inhibitor EHNA (1 mM) to the axons. Retrograde BMP4 signaling was also blocked by application of the BMP receptor inhibitor dorsomorphin (DMP, 10 μM) to the cell body compartment, but not by application of the inhibitor to the axonal compartment.

(D) Overexpression of dynamitin impairs BMP4 retrograde signaling. Axonal BMP4 treatment induced a 2.5-fold increase of pSMAD (red, arrows) only in the nuclei of neurons not expressing dynamitin (arrows). However, the increase in pSMAD was not seen in neurons overexpressing dynamitin (indicated by nGFP expression, green, arrowheads). The graph shows the quantification.

(E) Retrograde trafficking of biotinylated BMP4 from axons to the soma. Application of biotinylated BMP4 (20 ng/ml) to axons for 1 hr resulted in prominent anti-biotin immunofluorescence signals in the cell body (red). As controls, application of biotinylated BSA (20 ng/ml) or vehicle (PBS/borate/glycine) resulted in only baseline labeling in cell bodies.

For quantification, all data are mean ± SEM, n = 3 replicates. Between 100–200 cells were analyzed for each condition in each experiment. ns, not significant, **p < 0.01, *p < 0.05, compared with axonal BMP4 treatment group as indicated (B and C) or vehicle treatment

group (D), post hoc Tukey test after one-way ANOVA. Scale bars represent 20 μm (A); 10 μm (D and E).

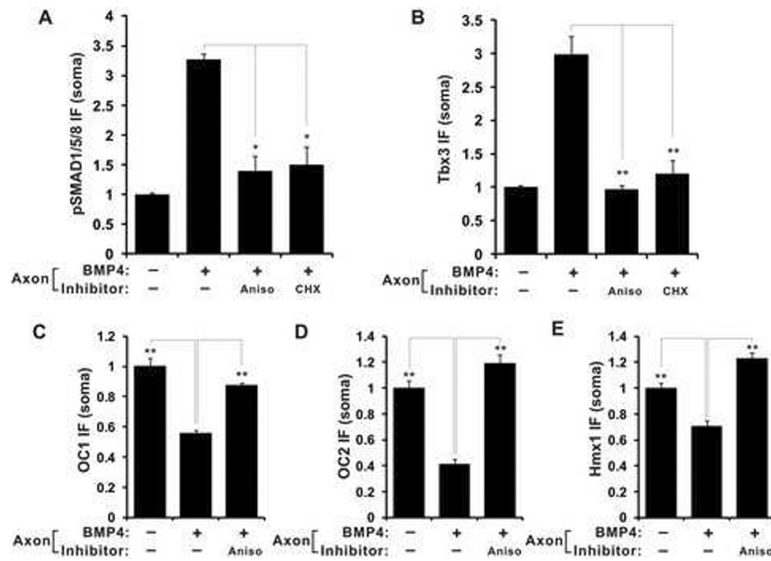


Figure 2. Retrograde BMP4 Signaling Requires Intra-Axonal Protein Synthesis

(A and B) Retrograde BMP4 signaling requires intra-axonal protein synthesis. The increase in nuclear pSMAD1/5/8 (A) and Tbx3 (B) induced by axonal BMP4 application were inhibited by inclusion of protein synthesis inhibitors anisomycin (Aniso, 200 μ M) or cycloheximide (CHX, 10 μ M) in the axonal compartment. Protein synthesis inhibitors and BMP4 were added to the axonal compartment at the same time.

(C–E) Repression of OC1, OC2 and Hmx1 retrograde BMP4 signaling requires intra-axonal protein synthesis. Application of BMP4 to the axonal compartment for 4 hr leads to a decrease in OC1 (C), OC2 (D) and Hmx1 (E) levels in the cell body by 44.3% (OC1), 60.0% (OC2) and 29.4% (Hmx1), respectively. The decrease in OC1, OC2 and Hmx1 levels in the cell body were inhibited by inclusion of protein synthesis inhibitor anisomycin (Aniso) in the axonal compartment.

For quantification, all data are mean \pm SEM, $n = 3$ replicates. Between 100–200 cells were analyzed for each condition in each experiment. ** $p < 0.01$, * $p < 0.05$, compared with axonal BMP4 treatment group as indicated, post hoc Tukey test after one-way ANOVA.

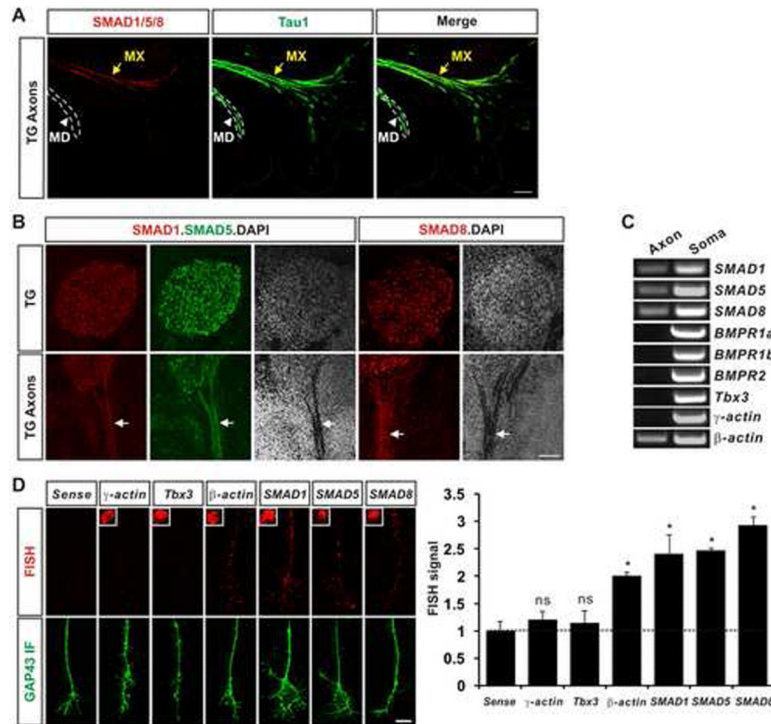


Figure 3. SMAD Protein and mRNA Are Localized to Axons of Trigeminal Ganglia Neurons
 (A) SMAD1/5/8 immunohistochemistry (red) reveals high levels in the maxillary (MX) projections (arrows) of trigeminal ganglia (TG), but not in the mandibular (MD) projections (outlined by white dotted line, arrowhead). Axon bundles were visualized by Tau1 immunofluorescence (green).
 (B) Expression of SMAD1, 5, and 8 in cell bodies and axons of trigeminal ganglia (TG) neurons. Immunohistochemistry of E13.5 rat embryo sagittal sections using specific antibodies against individual SMAD1, 5 and 8 isoforms shows SMAD protein in trigeminal ganglia cell bodies (upper panels). Each SMAD isoform was also detected in the maxillary axon bundles (lower panels, arrows). DAPI signal is excluded from axon bundles.
 (C) *SMAD1*, 5, and 8 transcripts are detected in the distal axons of trigeminal neurons. *SMAD1*, 5 and 8 mRNA were detected by RT-PCR using RNA harvested from the distal axon and neuronal soma, respectively. *BMPR1a*, *BMPR1b*, *BMPR2* and *Tbx3* transcripts were not detected in axons. β -actin is the positive control for axonal localization, and γ -actin was used as a negative control to exclude the possibility of contamination of the axonal fraction with cell body-derived material. All transcripts were detected in the trigeminal cell bodies.
 (D) Localization of *SMAD1*, 5, and 8 and 8 transcripts to axons by fluorescence in situ hybridization (FISH). Dissociated E13.5 rat trigeminal ganglia neurons were cultured for 2 DIV. *SMAD1*, 5, 8 and β -actin transcripts were detected in trigeminal axons in a characteristic punctate localization (red) typically seen with axonal transcripts (Lin and Holt, 2008). The control transcript, γ -actin, as well as *Tbx3*, exhibited similar minimal reactivity as observed with a sense *SMAD1* probe. GAP43 immunostaining (green) was used to visualize axonal borders. Insets, FISH labeling in the cell bodies of trigeminal neurons. The graph shows the quantification. Bars indicate mean \pm SEM, n = 3 replicates. A minimum of 15 axons for each probe was analyzed. ns, not significant, *p < 0.05 (compared with sense probe group, post hoc Tukey's test after one-way ANOVA). Scale bars represent 100 μ m (A and B); 10 μ m (D).

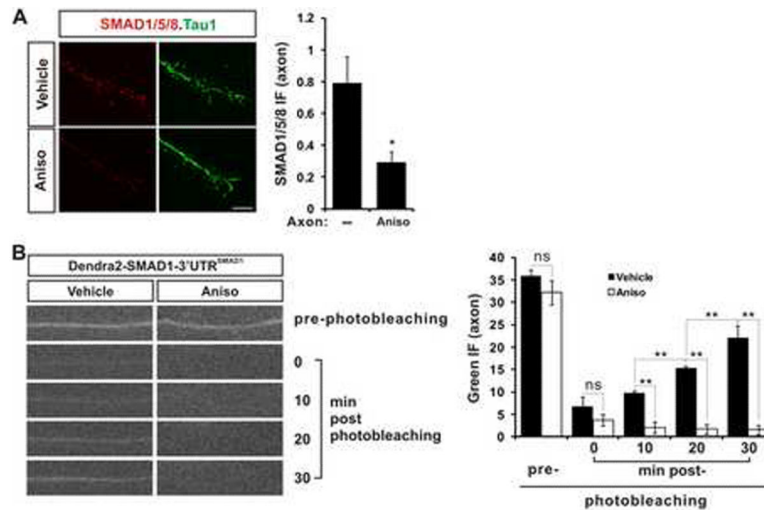


Figure 4. SMAD1/5/8 Is Locally Synthesized in Axons

(A) Axonal levels of SMAD1/5/8 are dependent on axonal protein synthesis. Application of anisomycin (Aniso, 200 μ M) to the axonal compartment for 4 hr resulted in a 62.8% reduction of axonal SMAD1/5/8 (red) protein levels. SMAD1/5/8 fluorescence intensity was normalized to the area defined by Tau1 fluorescence in the distal 50 μ m of the axon, including the growth cone.

(B) FRAP (fluorescence recovery after photobleaching) analysis of Dendra2-SMAD1 in axons. pDendra2-SMAD1-3'UTR^{SMAD1} was transfected into E13.5 trigeminal neurons and axons were severed from the cell body after 2 DIV. Expression of the fusion protein in axons was detected by its green fluorescence. Photobleaching was carried out in the distal axon (> 500 μ m from soma), which resulted in a near complete elimination of green signals. The recovery of green Dendra2-SMAD1 signal after photobleaching was monitored by live-cell imaging. A gradual appearance of green signal was observed, which increased 3.2-fold by 30 min. This recovery was blocked by treatment with anisomycin. The graph shows the quantification of green signal recovery.

For quantifications, bars indicate mean \pm SEM, n = 3 replicates. More than 20 axons for each treatment were analyzed. ns, not significant; *p < 0.05 (unpaired, two-tailed t test; panel A); **p < 0.01 (post hoc Tukey's test after one-way ANOVA as indicated; panel B). Scale bars represent 10 μ m.

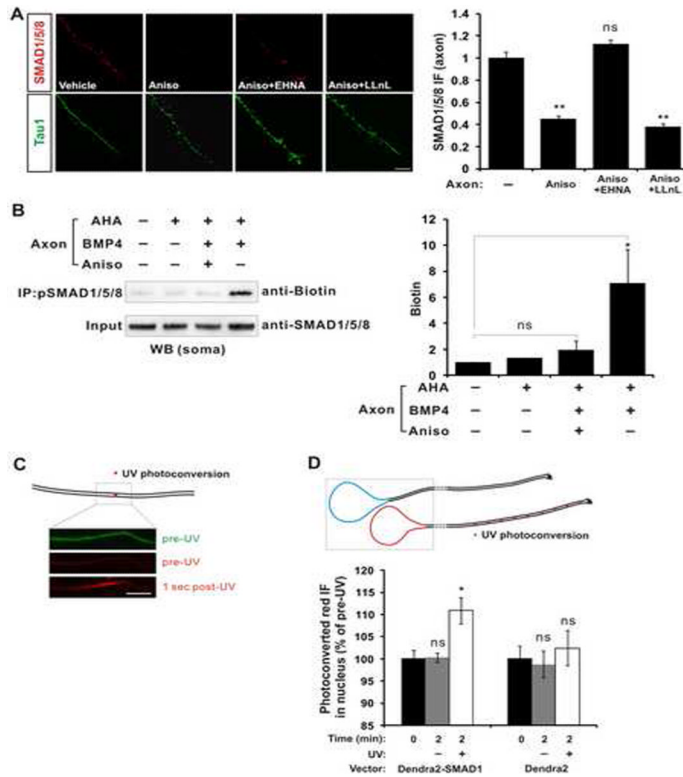


Figure 5. SMAD1/5/8 Retrogradely Traffics from Axon to Soma

(A) Time-dependent depletion of SMAD1/5/8 from axons is mediated by molecular motors. E13.5 rat trigeminal explants were cultured and axons were severed from the cell body after 2 DIV. A 55.4% loss of SMAD1/5/8 immunofluorescence intensity in the severed axons was observed after 1 hr treatment of anisomycin compared with vehicle. EHNA, but not LLnL, blocked the reduction of axonal SMAD1/5/8 levels. All experimental conditions included BMP4. Scale bar represents 10 μ m.

(B) Locally synthesized SMAD1/5/8 protein is retrogradely trafficked back to cell body. L-azidohomoalanine (AHA) was added to the axonal compartment to label the axonally synthesized proteins. Axons were treated with anisomycin or BMP4, as indicated. Lysates were collected from cell body compartments and immunoprecipitation with anti-pSMAD1/5/8 antibody was carried out, followed by Click-iT reaction to biotinylate AHA-labeled proteins. Anti-biotin western blotting detected AHA-labeled pSMAD1/5/8 in the cell body compartment. Levels of axonally derived pSMAD1/5/8 were increased upon axonal application of BMP4, while reduced levels were detected upon axonal application of anisomycin. The quantification is shown on the right.

(C) Photoconversion of Dendra2-SMAD1 in axons. pDendra2-SMAD1-3'UTR^{SMAD1} was transfected into E13.5 trigeminal neurons. Expression of the fusion protein was detected by its green fluorescence. After photoconversion of a 1- μ m segment (> 500 μ m from soma) in the axon by 0.1 sec irradiation with a 406 nm laser, the photoconverted signal was detected (red). Scale bar represents 10 μ m.

(D) Translocation of Dendra2-SMAD1 protein from the axon to the nucleus. pDendra2-SMAD1-3'UTR^{SMAD1} and pDendra2 expression constructs were transfected into E13.5 trigeminal neurons respectively. After photoconverting ~20 1- μ m segments (> 50 μ m from soma) in axons on DIV2, the accumulation of red signal in nucleus was measured 2 min later. To control for nonspecific photoconversion during imaging of Dendra2 or Dendra2-SMAD1 in neuronal nuclei, non-photoconverted neurons in the same microscopic field as the photoconverted neurons were used as controls. Photoconversion of Dendra2-SMAD1 in

axons resulted in a significant increase in photoconverted Dendra2-SMAD1 in the nucleus, compared with Dendra2.

For quantifications, bars indicate mean \pm SEM, n = 3 replicates. More than 20 axons (A) and neurons (D) for each treatment were analyzed. ns, not significant, *p < 0.05, **p < 0.01 (post hoc Tukey's test after one-way ANOVA compared with the vehicle treatment group in panels A and B, and 0 min timepoint group in panel D).

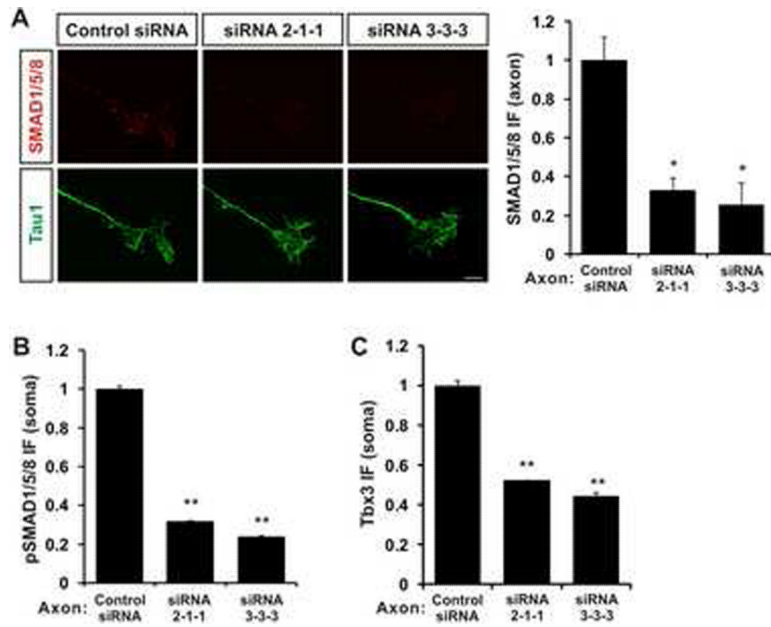


Figure 6. Retrograde BMP4 Signaling Requires Axonally Synthesized SMAD1/5/8

(A) Selective depletion of *SMAD1/5/8* from distal axons. Both siRNA cocktails (siRNA 2-1-1 and 3-3-3), containing siRNAs specific to individual *SMAD1*, 5 and 8 mRNAs, lead to a significant reduction (by 67–75%) in axonal SMAD1/5/8 (red) protein levels compared with a non-targeting siRNA control. Tau1 staining (green) was used to define the borders of axons and growth cones for fluorescence measurements. Scale bar represents 10 μ m.

(B and C) Retrograde BMP4 signaling is impaired following axonal knockdown of *SMAD1*, 5, and 8. Knockdown of axonal *SMAD1*, 5, and 8 inhibited BMP4-mediated retrograde induction of pSMAD1/5/8 by 68–76% (B) and Tbx3 by 51–62% (C).

For quantification, all data are mean \pm SEM, n = 3 replicates. Between 100–200 cells (B and C) and more than 15 axons (A) were analyzed for each condition. ns, not significant, **p < 0.01, *p < 0.05 (compared with control siRNA group, post hoc Tukey's test after one-way ANOVA).

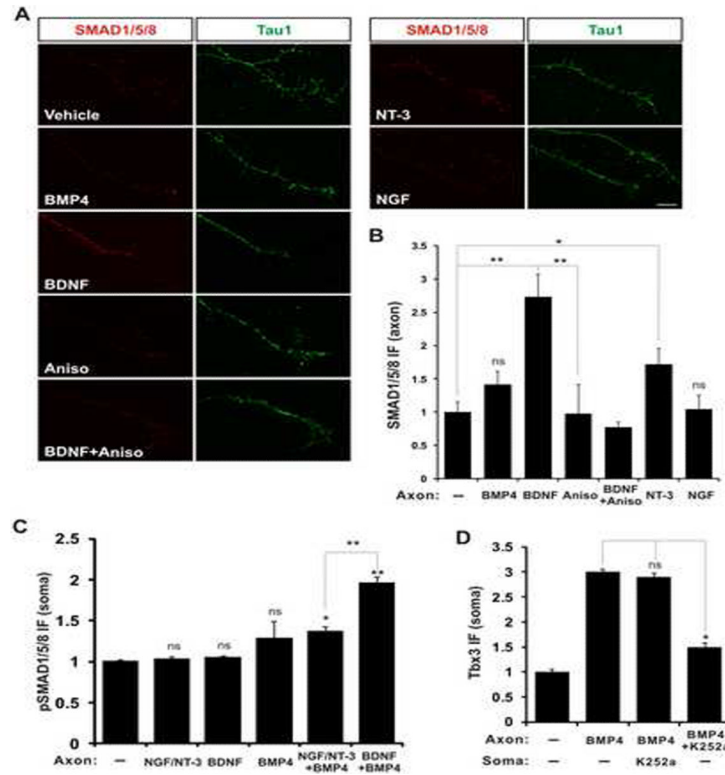


Figure 7. BDNF Acts Locally to Regulate SMAD1/5/8 Translation and Retrograde BMP4 Signaling

(A) BDNF induces intra-axonal synthesis of SMAD1/5/8. E13.5 trigeminal explants were grown in microfluidic chambers for 2 days, and then neurotrophin-free media was applied to the axonal compartment for 24 hr. Axons were then severed to ensure that any increase in SMAD1/5/8 levels do not derive from transport from the soma. Axons were treated with BMP4 (20 ng/ml), BDNF (25 ng/ml), anisomycin (Aniso, 200 μ M), NT-3 (50 ng/ml) or NGF (50 ng/ml) for 30 min. In untreated axons, SMAD1/5/8 (red) levels are nearly undetectable. However, SMAD1/5/8 levels increase significantly upon application of BDNF. This increase is blocked by anisomycin, indicating that the increase in SMAD1/5/8 levels derives from an increase in local translation. Substantially less or no induction was seen following treatment with other neurotrophins or BMP4. Tau1 staining (green) was used to define the borders of axons and growth cones for fluorescence measurements. Scale bar represents 10 μ m.

(B) Quantification of results in (A). BDNF induced a 1.7-fold increase in axonal SMAD1/5/8 levels, which was blocked with anisomycin. NT-3 induced a substantially smaller, although statistically significant 0.7-fold increase in axonal SMAD1/5/8 levels.

(C) Retrograde BMP4 signaling requires both BDNF and BMP4. Dissociated E13.5 trigeminal neurons were cultured in microfluidic chambers for 2 days, and then the media was switched to neurotrophin-free media for 4 hr. Axons were treated with NGF/NT-3, BDNF, or BMP4, alone and in combination for 1 hr, and nuclear pSMAD1/5/8 was measured by immunofluorescence. Retrograde induction of pSMAD1/5/8 was not elicited by axonal application of NGF/NT-3, BDNF or BMP4 alone, but was only observed when both neurotrophins and BMP4 were applied to axons. Nuclear pSMAD1/5/8 levels increased by 96.1% following axonal application of both BDNF and BMP4, and by 36.6% after axonal application of both NGF/NT-3 and BMP4.

(D) BDNF functions locally to regulate retrograde BMP4 signaling. Retrograde BMP4 signaling was blocked following axonal application of K252a (2 μ M), but not application of K252a to the cell body. BDNF was present in the culturing media. For quantification, all data are mean \pm SEM, n = 3 replicates. Between 100–200 cells (C and D) and more than 15 axons (B) were analyzed for each condition. ns, not significant, *p < 0.05, **p < 0.01, compared with vehicle (B, C) or axonal BMP4 treatment (D) group as indicated, post hoc Tukey's test after one-way ANOVA.

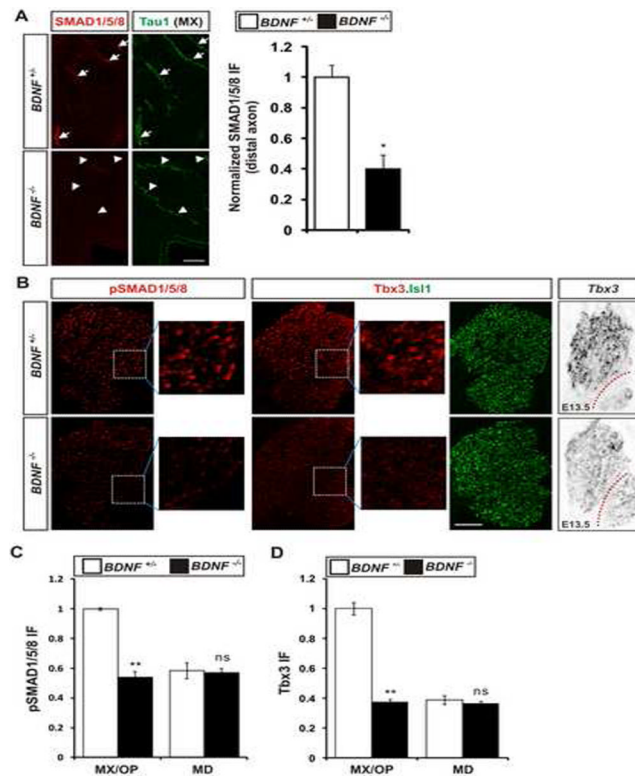


Figure 8. Loss of Axonal SMAD1/5/8 Protein and Trigeminal Ganglia Positional Identity Markers in *BDNF*^{-/-} Embryos

(A) Loss of SMAD1/5/8 in maxillary (MX) axons in *BDNF*^{-/-} embryos. BDNF is expressed in the maxillary and ophthalmic target fields of the trigeminal ganglia. SMAD1/5/8 (red) is readily detectable in the maxillary axonal projections (arrows) of the trigeminal ganglia in E12.5 *BDNF*^{+/+} mouse embryos. However, axonal SMAD1/5/8 staining is significantly reduced in *BDNF*^{-/-} embryos (arrowheads), indicating a role for BDNF in regulating axonal SMAD1/5/8 levels. Axon projections were visualized by Tau1 immunofluorescence (green). The quantification shows that SMAD1/5/8 labeling was decreased by 60.0% in the axon projections of *BDNF*^{-/-} embryos compared to *BDNF*^{+/+} littermates.

(B) Loss of pSMAD1/5/8 and Tbx3 expression in the trigeminal ganglia in *BDNF*^{-/-} embryos. Expression of both markers is readily detected in sections of the trigeminal ganglia from E12.5 *BDNF*^{+/+} embryos. However, expression of both markers is essentially abolished in *BDNF*^{-/-} embryos. Induction of *Tbx3* mRNA was also assessed at E13.5 by in situ hybridization. *Tbx3* transcripts were readily detected in *BDNF*^{+/+} embryos but not in *BDNF*^{-/-} embryos. Trigeminal neuron cell bodies were visualized by Is11 immunofluorescence (green). Is11 staining was used to identify neuronal nuclei for quantification of pSMAD1/5/8 and Tbx3 (C and D) and to confirm normal trigeminal ganglia formation in *BDNF*^{-/-} embryos. A portion of the trigeminal ganglia is shown at higher power to demonstrate changes in staining intensity in the nucleus. The red dotted lines indicate the boundary between the maxillary/ophthalmic (MX/OP) and mandibular (MD) regions of the trigeminal ganglia.

(C and D) Quantification of loss of pSMAD and Tbx3 expression seen in (B). Nuclear pSMAD1/5/8 and Tbx3 signals were quantified in maxillary and ophthalmic regions (MX/OP) and mandibular (MD) regions of trigeminal ganglia. Is11 labeling was used as a mask to demarcate the borders of neuronal nuclei for quantification. Nuclear pSMAD (C) and Tbx3 (D) expression in MX/OP of *BDNF*^{-/-} embryos was reduced by 46.2% and Tbx3 by 62.4%, to the low baseline levels seen in the MD region of the ganglia. The expression of these

markers in the MD portion of the trigeminal ganglia was not affected in the *BDNF*^{-/-} embryos.

For quantifications (A, C and D), all data are mean \pm SEM, n = 3 replicates. Between 4–5 sections were analyzed for each genotype. ns, not significant, *p < 0.05, **p < 0.01, unpaired, two-tailed *t* test. Scale bars represent 50 μ m (A); 100 μ m (B).